RJC

RASĀYAN *J. Chem.*
Vol. 18 | No. 3 |1541-1548| July-September | 2025
ISSN: 0974-1496 | e-ISSN: 0976-0083 | CODEN: RJCABP
http://www.rasayanjournal.com
http://www.rasayanjournal.co.in

AN ANALYSIS OF PB(II) ION REMOVAL FROM AQUEOUS SOLUTIONS EMPLOYING VARIOUS IRON TITANATE (FETIO3) NANOPARTICLE COMPOSITIONS

Jaya Ranga Rao Prathipati[1], T. Rambabu[2], Ravi Kota[3], Satheesh Ampolu[4], Sow Bhagyalakshmi Matcha[5], P. V. S. K. Phanidhar Varma[3], Nagakrishna Taidala[6] and T. Narasimhulu[1,✉]

[1]Baba Institute of Technology and Sciences, Visakhapatnam-530048, AP, India
[2]Dr. B. R. Ambedkar Gurukulam, Visakhapatnam -530047, AP, India
[3]Sanketika Vidya Parishad Engineering College, Visakhapatnam-530048, AP, India
[4]Centurion University of Technology and Management, Vizayanagaram-535216, AP, India
[5]College of Engineering (A), JNTUGV, Vizianagaram-535003, AP, India
[6]MRAGR Govt. Polytechnic College, Vizianagaram-535002, AP, India
✉Corresponding author: narsim.223@gmail.com

ABSTRACT

Iron titanate ($FeTiO_3$) nanoparticles were synthesised with three distinct Ti weight percentages and a constant Fe weight. These characterised nanoparticles were utilised as adsorbents to extract lead (II) from aqueous solutions. An atomic absorption spectrophotometer (AAS) was used to estimate the percentage of ion elimination. In all investigations, $FeTi^{-2.0}$ NPs showed efficient adsorption behaviour (SBET =199.1 m^2g^{-1}) for the removal of Pb (II) ions. The Nano catalyst had the highest adsorption capacity (qe, mg/g) in the Freundlich adsorption isotherm, and when the temperature (K) increased, the highest adsorption capacity was seen at 333 K (60°C). The adsorption process was found to be spontaneous and endothermic (ΔG^o = -8.43 kJ/mole; ΔH^o = 7.88 kJ/mole) under established conditions.

Keywords: Adsorption Isotherm, Thermodynamics, Wastewater Treatment, Nanoparticles, Chemical Oxygen Demand.

RASĀYAN*J. Chem.*, Vol. 18, No.3, 2025

INTRODUCTION

In the manufacturing process of fertilizers, pesticides, and several other agro products, the effluents that are discarded into the environment mainly contain toxic metal pollutants that can have adverse effects. These heavy metals, too, have their threshold limits (TLV), and exceeding these limits would cause severe biological impact on the aquatic flora and fauna. On the other hand, many of the metals act as essential body nutrients to human beings, and higher consumption would cause some disturbance in human health, like failure of the central nervous system, disorders in kidney and liver functions.[2] Therefore, it has become inevitable to eliminate the presence of toxic metals in the industrial discards before their disposal into the environment. Various strategies have been implemented by the researchers to eliminate these metal species, like chemical precipitation, reverse osmosis, coagulation, ion-exchange, ultra-filtration,etc.[4] These methods include few drawbacks like lower efficiency, sensitive experimental setup, operational challenges, and formation of toxic precipitates, which requires additional treatment methods.[5] Hence, it has become an important task for the industries and researchers to find an alternative technique for handling the treatment process. On analyzing various reports, it was observed that Adsorption is one of the facile and efficient treatment techniques in undertaking the wastewater remediation process[6]. Being an economical method, it was thoroughly implemented in various wastewater treatments. Activated carbon is one of the most investigated adsorbent materials, as it possesses a high specific surface area, stability, and cost-effectiveness. However, the material contains poor binding capacity due to the existence of randomly distributed adsorption sites on its surface.[8,9]As an alternative,

http://doi.org/10.31788/RJC.2025.1839148

some of the naturally available materials like red mud, clay, natural zeolites, etc, also contributed as efficient adsorbents.[10-13] Even though these materials are very economical and could bring out a better wastewater removal phenomenon, their availability, limited adsorption capacity of selected metal ions, and storage are major hurdles for many industries. Micro-organisms like bacteria, algae were also used as adsorbing species with acceptable results.[14]Another aspect of this research is the use of metal oxides or ferrites as adsorbents. Nickel ferrite ($NiFe_2O_4$) nanoparticles have recently been employed to remove hazardous metal ions from aqueous solutions, including Cr (VI), Pb (II), and Cd (II).[15] In the pH range of 3-7 and at 20-40 mg NPs weight, it was discovered that the elimination efficacy of Cr (VI), Pb (II), and Cd (II) was 89%, 79%, and 87%, respectively. Nano-magnetic Copper ferrite ($CuFe_2O_4$) adsorbents are effective in the removal of Pb(II) and Cd(II) ions from aqueous solutions with pH ranges of 5-10.[16] Ni-Cr ferrite NPs successfully eliminated Cr(VI) and Ni(II) ions from wastewaters at a pH of 9.0 at 70°C.[17]These materials are capable of decreasing metal ion concentrations; nevertheless, there are essentially no publications on experiments using iron titanates ($FeTiO_3$) NPs as adsorbents. These solid phase materials, composed of Fe^{+2}, Ti^{+4}, and O^{2-} ions, have been shown to have efficient magnetic characteristics.[18]They have an ilmenite phase in their crystal lattice, which is distinct from the typical ultraspinel titanium ferrites ($TiFe_2O_4$) (band gap = 2.3 eV).[19]As a result, the current study's goal was to create $FeTiO_3$ NPs with varying Ti weight percentages and a constant Fe content. Adsorption studies were carried out using these NPs to assess the ability to remove Pb (II) ions from aqueous solutions.

EXPERIMENTAL

Materials and Methods

Sigma Aldrich supplied all of the required chemicals (99% pure, AR grade). Lead (II) nitrate and Pb $(NO_3)_2$ were employed as metal ion solutions to investigate the removal of the corresponding metal ions from aqueous solutions. All of the necessary experimental solutions were produced with double-distilled water.

Synthesis of $FeTiO_3$ Nanoparticles

Mixing took place by combining 5 mL of 0.5 M iron nitrate, 2-3 mL of 0.5 M NaOH, and x mL of titanium isopropoxide (x 0.5, 1.0, 2.0) in three separate beakers (100 mL each). After this, the mixture was ultrasonicated for 40-60 minutes to ensure perfect mixing of the components. The materials were then heated at about 100-120 degrees Celsius to get rid of impurities and help the formation of ferrites, and then cooled to near room temperature. At about 5000 rpm, the mixtures were put through centrifugation, and the result was filtered, dried, and washed using a combination of ETOH and water. The dry powders were set at temperatures around 600-700°C and called $TiFe^{-0.5}$, $TiFe^{-1.0}$, and $TiFe^{-2.0}$ according to their respective volumes.

Instrumentation

All adsorption experiments were performed with a focal length of 250 mm, 1800 lines/mm diffraction grating, iCE Fios atomic absorption spectrophotometer (Thermo Fischer Scientific).

RESULTS AND DISCUSSION

Removal of Metal Ions from Wastewaters through Adsorption

The sample solutions for the experimental study were produced with a 0.1 N Pb(II) solution. The concentration of Mn^+ ions was determined by AAS, and the percentage removal of metals was estimated using eqn. (1).

$$\text{Percentage Removal of Metal Ion} = [(A-B)/A] \text{ X}100 \quad (1)$$

Where A and B are the metal ion concentrations before and after treatment with the NPs under the specified circumstances. Each experimental solution (50 mL) was placed in a 250 mL beaker, and a known amount of NPs (mg) was added. The combination was held under magnetic stirring (250 rpm) for a set period (min), and the resulting suspension was centrifuged (500 rpm), filtered, and the obtained supernatant liquid was analysed with AAS to determine the percentage removal of the respective metal ion in its solution.

The Impact of pH

The surface of these materials was discovered to be positive at pH < 4.4 and negative at pH > 4.4. By varying the pH of the aqueous metal solutions from 2.0 to 7.0 and distributing a known weight of $FeTiO_3$ NPs, the experimental solutions were magnetically agitated for a predetermined amount of time, and the AAS was used to detect the metal ion concentration in the solutions both before and after contact with the NPs. The findings were shown in Table-1, and the percentage removal of the metal was calculated using equation 1. The results show that as the pH of the solution increases, so does the percentage of elimination, up to pH 5.0. As a result, in these studies, it was determined that the synthesised $FeTiO_3$ NPs were effective at eliminating metal ions around pH 5.0. This behaviour was seen to develop gradually when the surface area of the NPs rose from $FeTi^{-0.5}$ to $FeTi^{-2.0}$. Increased surface area of the Nanocatalyst improves the rate of adsorption on its surface and optimises removal efficiency. Furthermore, adsorption was more successful at pH values lower than 5.0, indicating the presence of a positive charge on the surface of the $FeTiO_3$ NPs.

Table-1: Role of pH on the Removal of Pb (II)

pH	Metal ion	$FeTi^{-0.5}$	$FeTi^{-1.0}$	$FeTi^{-2.0}$
		% Removal		
2.0	Pb(II)	32%	48%	54%
3.0		49%	63%	79%
4.0		63%	80%	86%
5.0		78%	91%	93%
6.0		59%	79%	82%
7.0		42%	69%	70%

Effect of Adsorbent Weight

In the process of heterogeneous catalysis, the weight of the adsorbent plays a vital role in conducting the phenomenon. As it was identified, the $FeTiO_3$ NPs can display efficient catalytic activity in the pH range of 4.0 to 5.0. The role of adsorbent weight on the elimination of the ion was carried out by varying the composition of each nanocatalyst from 5 to 15 mg/L (Table-2). There was an increase in the removal of metal as the amount of catalyst increased from 5 to 15 mg/L of the solution. Besides, as the catalyst weight rose to between 20 and 30 mg/L, removing the contaminants proved more difficult. When the weights of the catalysts get higher, aggregation can occur and lead to lower activity of the catalyst. As a result, there is less ability of metal ions to adhere to the surface of $FeTiO_3$ NPs.

Table-2: Effect of Adsorbent Weight

Adsorbent Weight (mg)	Metal ion	$FeTi^{-0.5}$	$FeTi^{-1.0}$	$FeTi^{-2.0}$
		% Removal		
5	Pb(II)	39%	43%	45%
10		57%	65%	69%
15		68%	86%	89%
20		55%	68%	73%
25		50%	57%	67%
30		42%	58%	61%

Effect of Adsorbate Concentration

The rate at which metal ions (adsorbate) adsorb on the surface of $FeTiO_3$ NPs (adsorbent) is also affected by their concentration. Therefore, the investigation followed the main criteria given above, and the outcomes are shared in Table-3. As the concentration increased from 1 to 7 PPM, the rate of adsorption increased, but went down when the concentration was changed from 7 to 8 PPM. Higher solute concentrations decrease the number of active sites on the fixed weight of the catalyst, less and causes lower rate of adsorption.

Table-3: Effect of Adsorbate Concentration on the Removal of Pb(II)

Adsorbate con (PPM)	Metal ion	$FeTi^{-0.5}$	$FeTi^{-1.0}$	$FeTi^{-2.0}$
		% Removal		
1		35%	37%	43%
2		42%	51%	56%

3	Pb(II)	55%	71%	78%
4		63%	79%	83%
5		66%	81%	89%
6		67%	85%	90%
7		68%	87%	92%
8		56%	73%	79%

Impact of Contact Duration

Throughout the experiment, the pH was held at 5.0 with 0.1N HCl, and 15 mg of the nanocatalyst was put in all the testing solutions. The experiments were done by setting the contact time between 20 and 120 minutes with a 20-minute step difference at every trial. According to Table-4, there is an increase in the % removal of Pb (II) as the contact time between the $FeTiO_3$ NPs and the metal ions rises to 100 min. Yet, the percentage of removal drops by 100 min of contact time for all the $FeTiO_3$ NPs. It was noted from the results that after 100 min of interaction with all the $FeTiO_3$ NPs, the removal of metal ions was highly effective. In all the above experiments, the rate of adsorption has increased from $FeTi^{-0.5}$ to $FeTi^{-2.0}$ NPs with an increase in the surface area of the particles. Hence, in order to evaluate the tendency of the rate of adsorption, the adsorption isotherm was applied to the results with the NPs, and the results were discussed in the forthcoming sections.

Table-4: Effect of Contact Time for the Removal of Pb (II)

Contact Time (min)	Metal ion	$FeTi^{-0.5}$	$FeTi^{-1.0}$	$FeTi^{-2.0}$
		% Removal		
20	Pb(II)	34%	40%	43%
40		45%	52%	58%
60		52%	61%	68%
80		63%	70%	75%
100		78%	85%	89%
120		49%	69%	71%

Isotherm of Adsorption

A graph was made to show how the adsorbent's surface saturation and its equilibrium concentration change at a certain temperature. In the study, the Freundlich model was used to confirm the results of how fast Pb(II) is absorbed by $FeTi^{-2.0}$ NPs. The model can show how active sites are distributed on the catalyst's surfaces in an exponential way. It holds that multisite adsorption occurs, and eqn. (2) represents it linearly.

$$\ln q_e = \frac{1}{n}\, lnC_e + \ln K_F \qquad (2)$$

Where lnq_e and lnC_e denote the adsorbent's equilibrium adsorption capacity (mg/g $FeTiO_3$ NPs) and the adsorbate's equilibrium concentration (mg/L metal ion), respectively. The ln KF (Freundlich constant) was used to calculate the nanoparticles' adsorption capacity, intercept on the y-axis, with (1/n) representing the slope reflecting the NPs' surface heterogeneity. Figure-1 depicts a graph based on these inputs, with lnq_e on the y-axis and lnC_e on the x-axis at 303 K (30°C). This plot shows that the equilibrium adsorption capacity has risen from $FeTi^{-0.5}$ to $FeTi^{-2.0}$ for the removal of Pb(II) ions from its aqueous solution. The Freundlich constant (KF) increased significantly in proportion to the fraction of Ti in the NPs. These findings revealed that as the surface area of the NPs rose, so did their adsorption capacity. Furthermore, as shown in Table-5, the rate of adsorption increased when the temperature rose from 303K (30°C) to 333K (60°C). These findings can be attributed to the $FeTi^{-2.0}$ NPs' improved adsorption ability in the removal of Pb(II) ions from aqueous solutions. A. Heidari et al. reported that the adsorption capacity of NH^{2-} MCM-41 adsorbents is KF = 1.958, with n=1.095. At 298 K, the material effectively removed Pb (II), Cd (II), and Ni (II) ions from their aqueous solutions. Similarly, T. Yousefi et al. reported the efficient removal of Pb (II) ions using a modified zeolite adsorbent, whose adsorption capacity (KF, mg/g) decreased as temperature increased from 298 K to 333 K. At a lower temperature (298 K), the KF value was 30.6 mg/g, but it declined to 24.11 mg/g at 333 K. On the contrary, FeTi NPs demonstrated effective adsorption capability for the removal of Pb (II) ions, with a direct relationship between temperature and metal ion adsorption rate. At 333 K (60°C), the $FeTi^{-2.0}$ NPs had the maximum

adsorption capacity (q_e=36.12 mg/g) of all the synthesised NPs. As a result, the NPs were highly effective adsorbents for the removal of hazardous metals from wastewater, comparable to other efficient adsorbents.

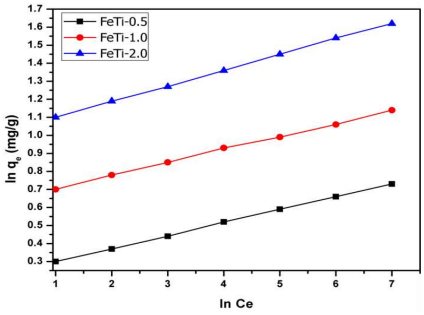

Fig.-1: Freundlich Adsorption Isotherm Plotted at 303 K (30 °C)

Table-5: Results of the Adsorption Capacity of the $FeTiO_3$ NPs

Adsorbent	Adsorption capacity, q_e (mg/g)			
	T=303K (30°C)	T=313K (40°C)	T=323K (50°C)	T=333K (60°C)
$FeTi^{-0.5}$	2.07 (lnq_e = 0.73)	5.72 (lnq_e=1.74)	8.77 (lnq_e=2.17)	13.17 (lnq_e=2.57)
$FeTi^{-1.0}$	3.12 (lnq_e = 1.14)	8.95 (lnq_e=2.19)	13.29 (lnq_e=2.58)	29.59 (lnq_e=3.38)
$FeTi^{-2.0}$	5.05 (lnq_e = 5.05)	11.95 (lnq_e=1.48)	25.32 (lnq_e=3.23)	36.12 (lnq_e=3.58)

Adsorption Thermodynamics

These experiments examine the exothermic (ΔH<0) or endothermic (ΔH>0), spontaneous (ΔG<0) or non-spontaneous (ΔG>0), and random (ΔS<0) or ordered (ΔS>0) adsorption of metal ions on the adsorbent surface (Milton). The temperature was varied between 303 K (30°C), 313 K (40°C), 323 K (50°C), and 333 K (60°C), and the related thermodynamic factors were calculated using eqns. (3) and (4).

$$\Delta G° = \Delta H° - T\Delta S° \quad (3)$$

$$\ln K_p = -\frac{\Delta Ho}{RT} + \frac{\Delta So}{T} = -\frac{\Delta Go}{RT} \quad (4)$$

Where G and H are the Gibbs free energy and enthalpy of the adsorption process (J/mol), S is the process entropy (J/mol/K), and T is the absolute temperature (Kelvin). The adsorption equilibrium constant, KP, was calculated from equation 5, where KF represents the adsorption capacity (from Freundlich adsorption isotherm), C is the initial concentration of the metal ion (mg/L), and γ is a dimensionless coefficient activity, which is assumed to be numerically equal to 1.0, as the samples under study were diluted.

$$K_p = \frac{K_F\, C}{\gamma} \quad (5)$$

As shown in the adsorption isotherm, the rate of adsorption has increased with increasing temperature. As a result, a graph was created depicting the adsorption capability of $FeTi^{-2.0}$ NPs (Fig.-2). The adsorbent's adsorption capability increased gradually as the temperature increased. It denotes that the rate of adsorption of Pb(II) ions on the surface of $FeTiO_3$ NPs is proportional to temperature, indicating that the process is endothermic. M. Manyangadze*et al.* postulated that a constant increase in adsorbent adsorption efficiency as temperature rises can result in an endothermic reaction. However, at very high temperatures (>60°C), the NPs' adsorption capability remained unchanged.

El-Naggar et al. reported the removal of Pb (II) ions using Kaolinite/Smectite natural composite adsorbents and found a linear relationship between adsorption rate and temperature from 303 K to 348 K. The results followed the Freundlich isotherm at pH around 2.0, with an ideal composite weight of 100 mg/L. Mustapha et al. tested powdered Albizia lebbeck pods to check how well Pb(II), Cd(II), Zn(II), and Cu(II) ions are absorbed from aqueous solutions. Trail studies at 353 K demonstrated that adsorption was efficient, and Langmuir can explain the phenomenon best. The reactions required the input of energy at low temperatures and happened easily at high temperatures. According to Gusain*et al.,* the MoS2/SH-

MWCNT nanocomposite was effective in adsorbing Pb(II) and Cd(II) ions. The technique was shown to be successful for removing both ions at temperatures around 328 K. The findings were analysed using the Freundlich isotherm model, which revealed that the process was both spontaneous (ΔG^o = -9 kJ/mol) and endothermic (ΔH^o = 8.06 kJ/mol). Similarly, Gao *et al.* reported the efficient removal of Pb (II) ions using Jujube Pit Biochar as adsorbents. They observed that the process was spontaneous at an average temperature of 303 K (ΔG^o = - 29.85 kJ/mol; ΔH^o = 22.520 kJ/mol). These scientific papers clearly show that the endothermic and spontaneous adsorption of Pb (II) ions on diverse adsorbents occurred at slightly higher temperatures. The adsorption phenomena exhibited by the $FeTiO_3$ NPs were endothermic (Fig.-2, Table-6), and the process was spontaneous as the temperature climbed from 303 to 333 K. The thermodynamic parameters were estimated using equations 4 and 5, and the results are shown in Table-6. The $FeTi^{-2.0}$ NPs had the highest spontaneity of the adsorption process (ΔG^o=-8.43 kJ/mole), and the endothermic nature was maintained with all NPs, with $FeTi^{-2.0}$ NPs having a higher endothermic nature (ΔH^o=7.88 kJ/mole).

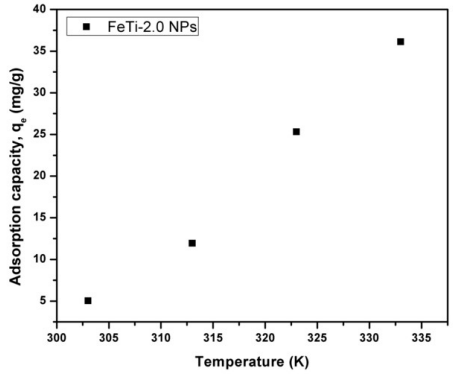

Fig.-2: Effect of Temperature on the Rate of Adsorption

Table-6: Thermodynamic Parameters

Nanoparticle	ln K_F	ln K_P	ΔG^o, kJ/mole	ΔH^o, kJ/mole
$FeTi^{-0.5}$	0.3	2.23	- 6.17	2.34
$FeTi^{-1.0}$	0.7	2.644	- 7.32	5.66
$FeTi^{-2.0}$	1.1	3.045	- 8.43	7.88

Studies on the Removal of Chemical Oxygen Demand (COD)

The chemical oxygen demand (COD) measurements were performed using a HACH DR/2010 Spectrophotometer equipped with a COD reactor, following the closed reflux, colorimetric method. The wastewater for the tests was obtained from Visakhapatnam's industrial regions (Pharma City, Aganampudi, Visakhapatnam, Andhra Pradesh, India), and the initial COD levels were determined using a diluted sample of a set value [10 ppm]. Based on the observed levels, the experiments were carried out using synthesised $FeTiO_3$ NPs and other predetermined conditions. The percentage COD loss was determined using equation 6.

$$\%\ COD\ loss = \frac{X-Y}{X}\ x\ 100 \qquad (6)$$

Where x and y represent the initial and end COD (mg/L) in the water sample under study, and the results are shown in Table-7.

Table-7: COD Studies with Various $FeTiO_3$ NPs

Time (min)	$FeTi^{-0.5}$		$FeTi^{-1.0}$		$FeTi^{-2.0}$	
	Y (mg/L)	% COD loss	Y (mg/L)	% COD loss	Y (mg/L)	% COD loss
15	984.3	3.6 %	723.6	29.16%	654.8	35.8%
30	765.4	25.07%	623.8	38.93%	423.7	58.5%
45	673.8	34.03%	512.1	49.86%	324.6	68.2%
60	567.09	44.48%	422.6	58.62%	231.8	77.3%
75	456.21	55.33%	355.1	65.23%	123.6	87.9%

90	324.7	68.2%	234.9	77.0%	98.76	90.3%
105	211.8	79.2%	178.5	82.5%	92.6	90.9%
120	201.6	80.2%	165.2	83.8%	85.6	91.6%

The initial COD (X, mg/L) of the obtained water sample was 1021.5 mg/L. The samples were examined under a colorimeter at 15-minute intervals, with three independent tests utilising $FeTi^{-0.5}$, $FeTi^{-1.0}$, and $FeTi^{-2.0}$ NPs (15 mg/L) scattered in solutions. The results show that the percentage of COD with $FeTi^{-0.5}$ NPs reached a maximum of 80.2% after 120 minutes. During the same period, the percentage COD loss with $FeTi^{-1.0}$ and $FeTi^{-2.0}$ NPs was 83.8% and 91.6%, respectively. These findings show that the NPs were efficient in decreasing the COD of polluted waterways.

CONCLUSION

The research describes the antibacterial uses of several acid-functionalised and metal-incorporated MCM-41 mesoporous materials. The PA-MCM-41 mesoporous material outperformed the SA-MCM-41 material in terms of antibacterial activity. Among the ingredients for Mn and Al-MCM-41, Mn-incorporated MCM-41 material showed greater effectiveness against the tested bacterial strains. A similar trend was observed in the antifungal activity against the tested fungal strains, leading to the conclusion that the synthesised MCM-41 with acid functionalisation and metal inclusion is mesoporous. The materials were physiologically active.

ACKNOWLEDGMENTS

The author is thankful to the authorities of the Engineering Chemistry Laboratory, Andhra University, Visakhapatnam, for providing the facilities to carry out the research work.

CONFLICT OF INTERESTS

The authors affirm that there is no conflict of interest with this article's publication.

AUTHOR CONTRIBUTIONS

The present work is related to *SDG-6: Clean Water and Sanitation*. All the authors contributed significantly to this manuscript, participated in reviewing/editing and approved the final draft for publication. The research profile of the authors can be verified from their ORCID ids, given below:

Jaya Ranga Rao Prathipati http://orchid.org/0000-0001-8561-1334
T. Rambabu http://orchid.org/0000-0003-2035-4634
Ravi Kota http://orchid.org/0009-0005-5550-8914
Satheesh Ampolu http://orchid.org/0000-0001-9191-3179
Sow Bhagyalakshmi Matcha http://orchid.org/0009-0004-3973-4498
P.V.S.K.PhanidharVarma http://orchid.org/0009-0002-2093
NagakrishnaTaidala http://orchid.org/0009-0008-7067-3434
T. Narasimhulu http://orchid.org/ 0000-0003-1519-0030

REFERENCES

1. A. Wang, Y. Si, H. Yin, J. Chen, J. H.Wang, *Materials Science and Engineering: B,* **249**, 114411(2019), https://doi.org/10.1016/j.mseb.2019.114411
2. Y. AlSalka, L. I. Granone, W. Ramadan, A. Hakki, R. Dillert, D. W. Bahnemann, *Applied Catalysis B: Environmental*, **244**, 1065(2019), https://doi.org/10.1016/j.apcatb.2018.12.014
3. Z. N. Garba, W. Zhou, M. Zhang, Z. Yuan, *Chemosphere,* **244**,125474(2020), https://doi.org/10.1016/j.chemosphere.2019.125474
4. V. K. Kermani, M. Schaffie, H. H. Rafsanjani, M. Ranjbar, *Hydrometallurgy,* **198**, 105507(2020), https://doi.org/10.1016/j.hydromet.2020.105507

5. Dresvyannikov, F. Alexander, O. Irina, Grigoryeva, R. Salemgaraeva, *Innovations in Corrosion and Materials Science,* **10**, 25(2020), https://doi.org/10.2174/2352094910666200225100537
6. M. Moradi, Y. Vasseghian, A. Khataee, M. Harati, H. Arfaeinia, *Separation and Purification Technology,* **261**, 118274(2021), https://doi.org/10.1016/j.seppur.2020.118274
7. J. E. Silveira, A. R. Ribeiro, J. Carbajo, G. Pliego, J. A. Zazo, J. A. Casas, *Water Research,* **200**, 117250(2021), https://doi.org/10.1016/j.watres.2021.117250
8. S. Shao, J. Yu, J. B. Love, X. Fan, *Journal of Alloys and Compounds,* **858**, 158388(2021), https://doi.org/10.1016/j.jallcom.2020.158388
9. G. Dong, L. Dong, K. Lang, D. Chai, D. Guo, Jinlong Li, M. Zhao, S. Chen, W. Zhang, *Journal of Environmental Chemical Engineering,* **10**, 108453(2022), https://doi.org/10.1016/j.jece.2022.108453
10. N. Subha, M. Mahalakshmi, S. Monika, P. SenthilKumar, V. Preethi, G. Vaishnavi, A. Rajabhuvanes wari, *Chemosphere,* **306**, 135631(2022), https://doi.org/10.1016/j.chemosphere.2022.135631
11. O. Tuna, Z. Balta, E. B. Simse, *Chemical Engineering Journal,* **474**, 145770(2023), https://doi.org/10.1016/j.cej.2023.145770
12. S. Narzary, K. Duraisamy, M. Nageswara, K. Chakraborty, S. Das, M. Gupta Choudhury, *Minerals,* **13(3)**, 406(2023), https://doi.org/10.3390/min13030406
13. L. Kasune, I. Munaweera, E. Sriyani, P. Kodithuwakku, N. Colin, *Advanced Materials Technologies,* **8(6)**, 2201292(2023), https://doi.org/10.1002/admt.202201292
14. S. Arunmetha, N. R. Dhineshbabu, K. Sakthipandi, *Journal of Materials Science Mater Electron,* **35**, 1793(2024), https://doi.org/10.1007/s10854-024-13566-5
15. S. Narzary, K. Duraisamy, N. R. Medikondu, *Optimal Quant Electron,* **56**, 1665(2024), https://doi.org/10.1007/s11082-024-07418-z
16. A. Attia, E. Elshehy, H. El Nahas, *Brazilian Journa lof Chemical Engineering*, **42**, 657(2024), https://doi.org/10.1007/s43153-024-00467-7
17. B. G. Park, *Transition Metal Chemistry,* **49(6)**, 439(2024), https://doi.org/10.1007/s11243-024-00595-6
18. C. Miranda, S. O. Rojas, C. Martínez, *Journal Mater Science,* **59**, 13772(2024), https://doi.org/10.1007/s10853-024-09940-7
19. Mohamed Jaffer Sadiq Mohamed , Mohammed A. Gondal, *Journal of Alloys and Compounds,* **1002**, 175382(2024), https://doi.org/10.1016/j.jallcom.2024.175382

[RJC-9148/2024]